# On the changing role of the stratosphere on the tropospheric ozone budget: 1979-2010

**P.T. Griffiths[1,2], J. Keeble[1,2], Y.M. Shin[1], N.L. Abraham[1,2], A.T. Archibald[1,2] and J.A. Pyle[1,2]**

[1]Chemistry Dept, Cambridge University, Lensfield Road, Cambridge, U.K.

[2]National Centre for Atmospheric Science, Cambridge University, U.K.

Corresponding author: Paul Griffiths (paul.griffiths@ncas.ac.uk)

## Abstract

We study the evolution of tropospheric ozone over the period 1979-2010 using a chemistry-climate model employing a stratosphere-troposphere chemistry scheme. By running with specified dynamics, the key feedback of composition on meteorology is suppressed, isolating the chemical response. By using historical forcings and emissions, interactions between processes are realistically represented. We use the model to assess how the ozone responds over time and to investigate model responses and trends. We find that the CFC-driven decrease in stratospheric ozone plays a significant role in the tropospheric ozone burden. Over the period 1979-1994, the decline in transport of ozone from the stratosphere, partially offsets an emissions-driven increase in tropospheric ozone production. From 1994-2010, despite a levelling off in emissions increased stratosphere-to-troposphere transport of ozone drives a small increase in the tropospheric ozone burden. These results have implications for the impact of future stratospheric ozone recovery on air quality and radiative forcing.

## Plain language summary

We use a modelling approach to study the effect of stratospheric ozone depletion on the composition of the troposphere. We focus on the period 1979-2010 and use a chemistry-climate model employing historical emissions, climate forcing and meteorology. Our model has a good description of both stratospheric and tropospheric ozone chemistry and allows us to calculate the effect of exchange between stratosphere and troposphere. We show that stratospheric ozone depletion over the period 1979-2010 has a critical effect on tropospheric composition – with less ozone in the lower stratosphere, there is less transport to the troposphere, and this offsets an emissions-driven increase in ozone production in the troposphere. Such combined studies are important to quantify the future effects of stratospheric ozone recovery on the evolution of tropospheric composition.

## Introduction

The changes in tropospheric ozone since the pre-industrial era are estimated to have resulted in an increase in radiative forcing of 0.4 W m$^{-2}$ (Stevenson et al., 2013, Myhre et al., 2013),  making tropospheric ozone the third most important anthropogenic greenhouse gas.  Unlike the major greenhouse gases, carbon dioxide ($CO_2$) and methane ($CH_4$), ozone is not emitted directly, but is the result of the oxidation of VOCs in the presence of $NO_x$ (Monks et al., 2015).  The tropospheric ozone abundance is controlled by a balance of sources, including photochemical production ($P_{O3}$) and downward transport of ozone-rich air from the stratosphere ($S_{O3}$), and sinks, principally physical losses at the surface (deposition, $D_{O3}$) and chemical loss throughout the free troposphere ($L_{O3}$).

Ozone has important impacts on vegetation and human health.   In addition, ozone is important since it indirectly affects the lifetime of other greenhouse gases, particularly methane, through its role in the formation of the hydroxyl radical (OH) (Voulgarakis et al., 2013).  OH and ozone also have an impact on aerosol radiative forcing, a major source of uncertainty in the climate system, as secondary aerosols such as sulfate, nitrate and secondary organic aerosol are mediated by tropospheric oxidants and play a major role in the aerosol budget and burden (Karset et al., 2018).  Therefore, ozone is linked throughout the Earth system, as changes in ozone can have knock on impacts on emissions of ozone precursors through feedbacks induced by changes in temperature and the hydrological cycle (driven by the changes in aerosols and clouds and radiative forcing), which themselves will modify ozone.

Measurements of ozone on a global scale are challenging, making modelling of atmospheric composition, and accurate model treatment of ozone production and loss, critical to our understanding of this important species. The International Global Atmospheric Chemistry (IGAC) Chemistry Climate Model Initiative  (Eyring et al., 2016; Morgenstern et al., 2017) provided a mechanism to coordinate multi-model simulations of the historic evolution of ozone in the troposphere and stratosphere and their future evolution out to the end of the 21st Century. Results from CCMI indicate that global mean stratospheric ozone is projected to return to 1980s levels between 2045-2059 (Dhomse et al., 2018) but that the timing of this return depends on the extent of greenhouse gas emissions. As a result of increased greenhouse gas abundances, tropical total column ozone is likely to decrease by the end of the century (Oman et al., 2010; Eyring et al., 2013; Keeble et al., 2017). Revell et al. (2018) highlight a large spread in the CCMI models tropospheric ozone columns, with a bias compared to OMI-MLS data for the year 2005 of ±14 Dobson Units (~ 50%). They go on to explore the causes of bias in tropospheric ozone in the SOCOL model through performing an extensive series of sensitivity studies highlighting a large sensitivity of the SOCOL model tropospheric column ozone to emissions of ozone precursors in the year 2000.   Abalos et al. (2019) focus on the role of changes in the stratospheric influx of ozone into the troposphere over the coming century and show that models agree that an acceleration of the stratospheric circulation driven by increases in greenhouse gas emissions will result in increased stratosphere-to-troposphere transport (STT).

While we have a good understanding of the current distribution of tropospheric ozone, owing to a large number of different measurements, our understanding of changes to the historic ozone burden and budget is less complete. The Tropospheric Ozone Assessment Report (TOAR) estimates that the tropospheric ozone burden averaged  over 2010-2014 is 302 (281–318) Tg (Gaudel et al., 2018).  This compares well with multi-model means (MMM) from model intercomparisons of 337±23 Tg (ACCMIP,(Young et al., 2013) ) and 336±27 (+16 - 21) Tg (ACCENT,(Stevenson et al., 2006) (although we note the TOAR burden is restricted to the latitude ±60˚).  What controls this burden is still under debate. The recent literature on the chemical production ($P_{O3}$) and loss ($L_{O3}$) of tropospheric ozone highlights a lack of data on the topic to make reliable assessments. $P_{O3}$ is estimated to be much larger than the source from the stratosphere ($S_{O3}$) in all model simulations which have calculated this (Young et al., 2018)  however there is wide-spread in the magnitude of $P_{O3}$. Young et al. (2018) review the spread in the tropospheric ozone budget terms for the year 2000 and highlight a factor of ~ 2 spread across each term ($P_{O3}$, $L_{O3}$, $S_{O3}$ and $D_{O3}$) with $S_{O3}$ and $D_{O3}$ having the highest spread between models. Whilst models agree that $P_{O3}>S_{O3}$ there is less agreement historically on the sign of $P_{O3}-L_{O3}$, with some models suggesting the troposphere is a net sink for ozone.

In this study we aim to understand how the budget of tropospheric ozone has evolved over the recent historical period. Our focus is 1979-2010 and our assessment is based on the results from an updated run from the CCMI nudged dynamics refC1SD simulation (Morgenstern et al., 2017). Our aim is to quantify the impact of changes in emissions of ozone precursors (and so the chemical source of tropospheric ozone) relative to the change in influx of ozone from the stratosphere over this time period. Our paper is arranged with a description of the

93 model and simulation set up (Section 2), a summary of the results of our analysis and a discussion of their
94 impacts on our understanding (Section 3). We finish with some conclusions on how future observations may
95 enable improved understanding of the role of stratospheric ozone trends on the troposphere.

## Method

97
98 Here we assess recent changes to the tropospheric ozone budget using version 7.3 of the Met Office Unified
99 Model, based on the science version HadGEM3-A configuration (Hewitt et al., 2011) coupled with the United
100 Kingdom Chemistry and Aerosol scheme, hereafter UKCA-StratTrop. The simulation follows the experimental
101 design of the IGAC/Stratosphere-troposphere Processes And their Role in Climate (SPARC) Chemistry-Climate
102 Model Initiative (CCMI) refC1SD experiment.   This simulation spans 1979-2010, with emissions taken from
103 MACCity (Granier et al., 2011), and uses prescribed sea surface temperatures and sea ice from HadISST
104 (Rayner et al., 2003). Horizontal wind components (u and v) and potential temperature ($\theta$) are nudged
105 (following (Telford et al., 2008)) to ERA-Interim Reanalysis data (Dee et al., 2011).  The meteorological
106 reanalysis includes dynamical effects of stratospheric ozone depletion and increased greenhouse gas
107 concentration, both of which enhance the speed of the Brewer-Dobson circulation (Abalos et al., 2019).
108
109 The chemical scheme used in UKCA-StratTrop is a combination of the tropospheric  (O'Connor et al., 2014) and
110 stratospheric  (Morgenstern et al., 2009) schemes.  By using historical emissions, sea surface temperatures and
111 meteorology we are able to accurately capture both the long-term tropospheric ozone changes (driven
112 predominantly by anthropogenic emissions) and short-term changes (e.g. those driven by ENSO, etc).  Further,
113 by using a combined stratosphere-troposphere chemistry scheme, the influence of stratospheric ozone changes
114 on the tropospheric ozone budget are more accurately represented.
115
116 A full understanding of recent changes to the tropospheric ozone burden requires detailed analysis of the
117 tropospheric ozone budget, including quantification of the chemical production and loss fluxes, stratosphere-
118 troposphere exchange and the deposition of ozone at the surface.  UKCA-StratTrop includes 85 tracers, with 83
119 involved in chemistry, 59 photolytic reactions, 199 bimolecular reactions and 25 uni- and ter-molecular
120 reactions.  The chemistry employs primary emissions of 12 species and dry and wet deposition of 39 and 14
121 species.  Heterogeneous reactions occurring in the troposphere on sulfate aerosols are included.  As a result, the
122 model includes state-of-the-art tropospheric ozone chemistry. Dry deposition is parameterised employing a
123 resistance type model (Wesely, 1989) using the implementation described in Archibald et al. (2019), while STE
124 is calculated using an online method every chemical timestep.
125
126 For the monthly mean data, the tropopause height was diagnosed using the WMO thermal tropopause, and a
127 mask applied to the reaction fluxes.  For this study we calculate ozone production and loss terms using sums of
128 reaction fluxes, similar to the methods used by Tilmes et al. (2016).  Ozone production is calculated as the
129 reaction flux through the rate-determining reactions, namely $HO_2+NO$, the sum of the various $RO_2+NO$
130 reactions involving peroxy radicals derived from methane, ethane, propane and isoprene, and the release of
131 peroxy radicals from organic nitrate photolysis, the reactions of OH with $RCO_2H$, organic nitrates and PAN.
132 Ozone chemical destruction is derived from $O^1D+H_2O$, $HO_2+O_3$, $OH+O_3$, ozonolysis of alkenes, as well as
133 indirect terms including loss of the Ox reservoirs, $N_2O_5$, and reaction of $NO_3$ with VOCs.  Dry deposition of $O_3$
134 and $NO_y$ species, as well as wet deposition of $NO_y$, are also included as ozone loss.

135 Table 1: tropospheric ozone budget terms, broken down into annual mean sum fluxes.  All quantities are given
136 in units of $Tg(O_3)$ per year for UKCA-StratTrop integrations for year 2000.
137

| Chemical O3 production / Tg per year | 4751 | Chemical destruction / Tg per year | 4193 |
|---|---|---|---|
| P1: HO2 + NO | 3185 | L1: O1D + H2O | 2205 |
| P2: CH3O2 + NO | 1092 | L2: HO2 + O3 | 1356 |
| P3: RO2 + NO | 345 | L3: OH + O3 | 518 |
| P4: OH + RCO2H | 18.9 | L4: O3 + ALKENE | 58.2 |
| P5: OH + RONO2 | 7.8 | L5: NO3 Loss | 50.0 |

| P6: OH + PAN | 45.9 | L6: N2O5 Loss | 6.6 |
|---|---|---|---|
| P7: RONO2 + hv | 1.8 | D1: Dry deposition O3 | 852 |
| P8: JO2 | 55.0 | D2+D3: Wet + dry deposition NOy | 147 |
| STE | 451 Tg | Residual (STE) | 441 |

138
139 From the table above, it can be seen that the residual STE of ozone, calculated from the budget as STE =
140 $L_{O3}+D_{O3}-P_{O3}$ agrees with the diagnosed online STE of ozone to within 2%. When making budget calculations,
141 the table shows that it is important to include the contribution from photolysis of molecular oxygen in the upper
142 tropical troposphere, which is of the order of 10% of this residual contribution, with its inclusion closing the
143 budget to within 2%, consistent with the findings of (Prather, 2009). The model terms compare well with
144 (Tilmes et al., 2016) for similar CCMI refC1SD experiments of $P_{O3}$=4693, $L_{O3}$=4256 and $D_{O3}$=871 Tg yr$^{-1}$ and
145 slightly lower but within the range of the ACCMIP mean values of 4937±656. 4442±570 and 996±203 Tg yr$^{-1}$
146 (Young et al., 2018). The residual STT of 441 Tg yr$^{-1}$ is within the ACCMIP range of 535 ± 161 Tg yr$^{-1}$ (Young
147 et al., 2013).
148
149 In order to assess the role of recent changes to the stratospheric ozone burden on the tropospheric ozone budget,
150 a second integration (fODS_LBC) was performed in which the lower boundary condition of all halogenated
151 ODS was kept constant at 1979 values, but all other forcings and emissions were allowed to evolve as in the
152 HIST experiment. Comparing fODS_LBC with the HIST simulations allows us to quantify the impacts of
153 stratospheric ozone decreases arising from the emission of halogenated ODS on tropospheric ozone. Both
154 simulations were nudged to the same meteorology, as this isolates the chemical effects of halogenated ODS, and
155 keeps the mass flux between the troposphere and stratosphere constant between the two experiments, ensuring
156 that any changes to STE are the result of stratospheric ozone burden changes.

## Results and Discussion

### Model performance for year 2000

159 Figure S1 shows a comparison of the tropospheric ozone column with OMI-MLS data, generated by applying a
160 tropospheric mask generated from a 125 ppbv ozonopause (Gaudel et al., 2018) . The UKCA-StratTrop model
161 accurately captures the observed seasonality, albeit with a slightly late onset of ozone in the NH and a slightly
162 early onset in the SH. The spatial structure compares well with the satellite observations, with the largest
163 differences occurring in the boreal summer in the extratropics. The area weighted mean TCO in UKCA-
164 StratTrop is 28.4 DU vs the OMI mean of 35.2DU. The mean ozone value is significantly closer to the
165 OMI/MLS mean than the configuration of the models employing UKCA used in the CCMI refC1 integrations,
166 analysed in (Revell et al., 2018), which, in contrast to the scheme used here, used a reduced complexity
167 tropospheric chemistry scheme that does not treat NMVOC. In that configuration, UM-UKCA showed the
168 lowest tropospheric ozone burden of the various models, with a low bias with respect to OMI/MLS of 14.1 DU
169 for 2005 (Figure 6 of Revell et al., 2018). For these experiments, the model bias is around 7 DU low,
170 highlighting the importance of the chemical scheme and the role of NMVOC in tropospheric ozone production.
171 It should be noted that the exact value of the bias also depends strongly on tropopause definition, with a lower
172 bias generally observed when using the WMO tropopause definition. The tropospheric $O_3$ burden averaged
173 from 60ºS to 60ºN (using 125 ppbv ozonopause) is 295 Tg for year 2000, which compares well with
174 observational estimates of between 280 Tg and 320 Tg (Gaudel et al., 2018), over the same latitude range. The
175 model whole troposphere burden for year 2000 is 320 Tg, which is in agreement with estimates from Young et
176 al. (2013) of 337 ± 23 Tg. Methane is forced by a lower boundary condition that follows CCMI historical
177 concentrations at the surface, from which we derive a tropospheric $CH_4$ burden of 5000 Tg and a lifetime with
178 respect to oxidation by tropospheric OH of 9.0 years, in good agreement with the ACCMIP mean $CH_4$ lifetime
179 of 9.3 +/- 0.9 years (Voulgarakis et al., 2013). The airmass-weighted tropospheric mean OH is $10.6\times10^5$ cm$^{-3}$
180 which agrees well with ACCMIP MMM of $(11.7\pm1.0)\times10^5$ cm$^{-3}$ (Naik et al., 2013).
181
182

Evolution of tropospheric ozone burden and budget 1979-2005

Figure 1 shows the evolution of the stratospheric and tropospheric burden for both the HIST and fODS_LBC integrations. It can be seen that in HIST there is a strong decrease in modelled stratospheric ozone over the period 1980-1995 as a result of the increased CFC concentrations in the stratosphere and accompanying ozone destruction via chlorine species . Stratospheric chlorine reaches a maximum in 1997 [Maeder et al., 2010], and in the mid 1990s the decline in stratospheric ozone burden ceases, and signs of recovery emerge over the next 10 years. Over this period, the trend in tropospheric ozone burden follows the behaviour in stratospheric ozone although less strongly and with a greater effect of interannual variability. In the fODS_LBC experiment, significantly less ozone depletion is calculated, although there is some decline as the stratospheric chlorine loading adjusts to the imposed 1979 constant lower boundary condition. This adjustment requires a period of around five years for the chlorine to be transported to high latitudes by the Brewer-Dobson circulation [Butchart, 2014]. In the HIST experiment, the trend in tropospheric ozone burden is slightly negative over the period 1980-1993, and is thereafter positive. In fODS_LBC, a different behavior is calculated, with no significant trend from 1980-1993, and a positive trend thereafter.
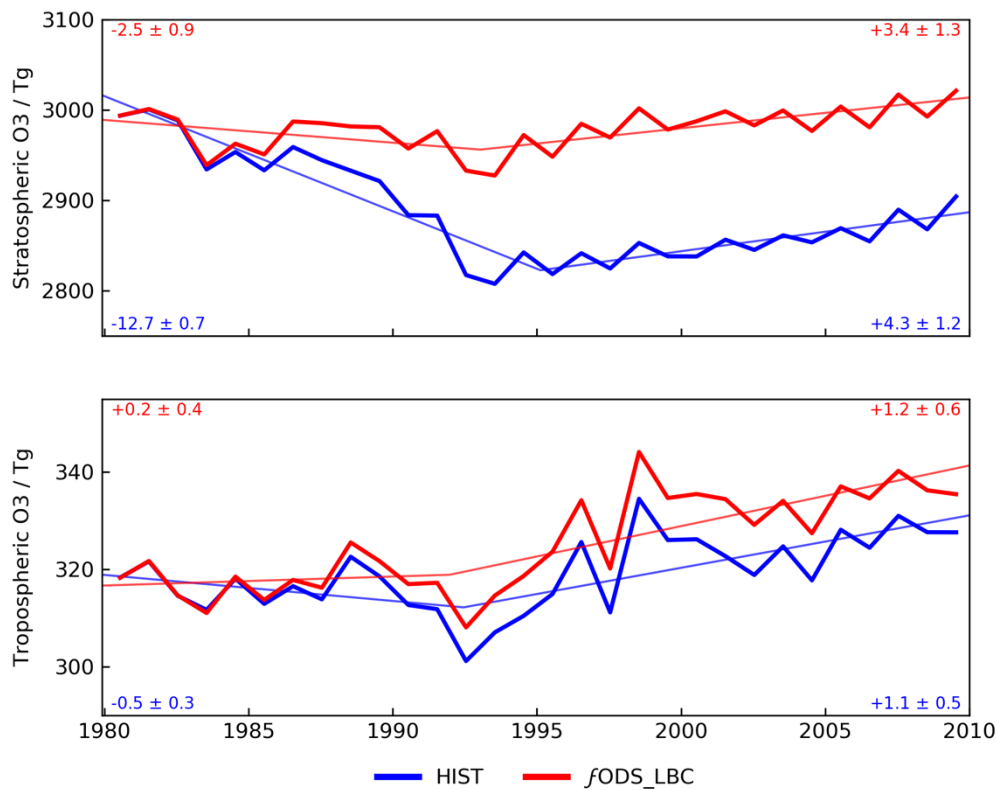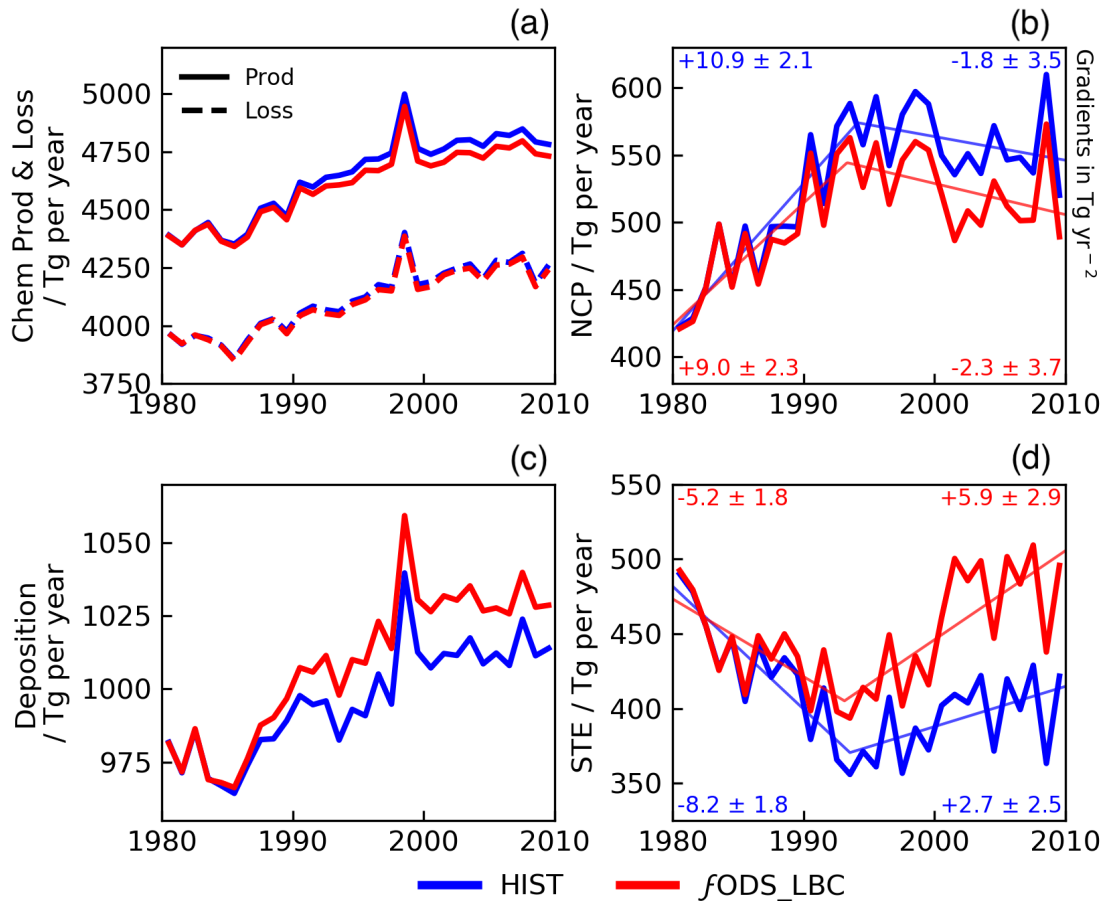


Figure 1 - Transient behaviour of annual mean stratospheric (a, upper) and tropospheric (b, lower) ozone burden.

Piecewise linear regression was used to determine the linear trends in burdens and fluxes, and these are shown in Figure 1. To fit the trends, least squares regression was used, with initial parameters determined by latin hypercube sampling, optimising using root mean square error. We find inflection points in the stratospheric burden at 1995 ($\pm$ 1 year) for the HIST run, and 1993 $\pm$ 1 at for fODS_LBC. For the troposphere, these inflection points are 1992 $\pm$ 2 for the HIST run, and 1992 $\pm$ 3 for fODS_LBC.

## Discussion

The MACCity emission data (Granier et al., 2011) used for these simulations describe an increase in emissions of tropospheric ozone precursors over the period 1979-2009 which leads to enhanced chemical production, particularly at the surface in the vicinity of key emissions hotspots. Deposition, which occurs via various processes close to the surface, also increases over this period, reflecting more closely the increase in ozone production, rather than the tropospheric burden. Increases in the ozone burden do lead to an increase in OH and $HO_2$, particularly in the free troposphere, with concomitant increase in chemical destruction via reactions L2 and L3.



Figure 2: behavior of the fluxes controlling the tropospheric ozone burden. a: Chemical production and loss. (b): Net ($P_{Ox}$-$L_{Ox}$) chemical production. (c): Deposition of Ox and NOy. (d): Net STT of ozone. Heavy lines show the annual means, and light lines show the piecewise linear fit. In (a), the solid line shows Ox chemical production, and the dashed line shows Ox chemical loss. Captions show gradient in Tg per year[2].

Figures 2a shows the behaviour in the gross global fluxes controlling the ozone burden in both HIST and fODS_LBC. Chemical production and loss were calculated as using reactions P1-P8 and L1-L6 respectively. Figure 2b shows the difference between these terms, Net Chemical Production (NCP), while Figures 2c and 2d show deposition and STE of ozone. The deposition describes the amount of Ox deposited in wet and dry deposition, and the STE encapsulates the net transport of ozone from the stratosphere into the troposphere.

In both simulations, there is some interannual variability, with other transient features also apparent. These are associated with modes of unforced climate variability, such as ENSO, with peak and trough in ozone production occurring around strong events in the mid 1980s and in 1997. These climate events are also present in the NOx and CO emissions used in CCMI refC1SD which represent the fire emissions from these events. Spikes in ozone chemical production, loss and deposition can be seen around 1997 which reflect the strong transient increase in emissions of ozone precursors in the MACCity emissions used for these simulations, and which

represent the increase in biomass burning that year, particularly around SE Asia.  We examined the effect of these events on the trends and find no statistically significant difference in trends when calculated when the El Nino years are ignored in the analysis.  Removing 1997 and 1998 from our data,  resulted in the early trend changing from –0.53 ± 0.34 Tg per year to –0.59 ± 0.31 Tg per year, and the later trend changing from +1.07 ± 0.52 Tg per year to +1.10 ± 0.48, identical within mutual uncertainty and showing that El Nino has no effect on the retrieved values for the tropospheric ozone burden trend over 1979-2010.  Although dynamical effects may also play a part (Voulgarakis et al., 2011), there is little evidence of a transient increase in STE in these integrations around this time.

Chemical production and loss of tropospheric ozone increase over the entire experiment.  In HIST, over the period 1979-1996, ozone production increases at a slightly faster rate than loss resulting in an increase in NCP over this period.  After 1996, losses increase slightly faster than production, leading to a smaller and slightly net negative trend in NCP.  This partially reflects the behaviour of the precursor emissions, which reach a maximum around 1995 and then decline after this point.  In HIST, photochemical production of ozone due to lower overhead ozone and higher photolysis rates [Voulgorakis et al., 2013] than in fODS_LBC.

STE of ozone (the transport of ozone from the stratosphere into the troposphere) declines sharply from 1979-1994, consistent with the decline in lower stratospheric ozone associated with the use and emission of halogenated ODS, particularly the CFCs, throughout this time. From 1994-2006, modelled STE slowly increases, driven in part by early signs of stratospheric ozone recovery in the mid-latitudes (e.g. (Keeble et al., 2018), and stratospheric dynamical changes resulting from increased GHGs (e.g.(Butchart, 2014)).  We note that these two effects are not isolated, with stratospheric ozone depletion and stratospheric dynamics closely coupled (e.g. Keeble et al. (2014, Polvani et al. (2018)).

In the fODS_LBC experiment, the STE term declines to a minimum in 1994, albeit at a slower rate than in HIST, before increasing from 1994 to the end of the integration.  The greater rate of increase in STE after 1994 in the fODS_LBC integration compared with HIST can be attributed to the higher stratospheric ozone burden in this experiment, as the stratosphere-to-troposphere mass transport is identical between simulations.  In fODS_LBC NCP is lower than in HIST, particularly as the stratospheric ozone burdens in the two experiments diverge and the photochemical ozone production in HIST increases.

Comparing HIST to fODS_LBC directly quantifies the chemical impacts of stratospheric ozone depletion on the tropospheric ozone budget.  Figure 3 shows the difference in NCP, STE and DD between the HIST simulation with respect to fODS_LBC.  The differences for each in the year 1980 are near zero, as the simulations start from the  same initial conditions.  They diverge after ~5 years, consistent with the time it takes for the surface ODS mixing ratios prescribed by the LBC to be transported into the polar stratosphere.  After 1985, STE is lower in the HIST simulation by around 75 Tg $yr^{-1}$ between 2000-2006, reflecting the lower stratospheric ozone burden, while NCP is up to 50 Tg $yr^{-1}$ higher, reflecting the increased photochemical production of ozone.  Deposition of ozone follows the tropospheric burden, and so is lower in the HIST simulation by ~20 Tg $yr^{-1}$.
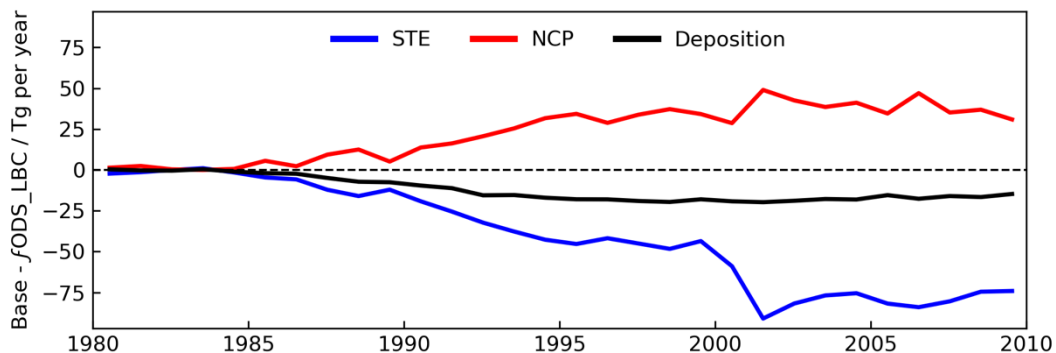


Figure 3: summary of HIST and fODS_LBC counterfactual experiments.  The different in budget terms is shown over the period of the integrations.  Data are shown as HIST-fODS_LBC.

285　In conclusion, the HIST integration represents our best estimate of past tropospheric ozone changes as it follows
286　historical emissions and meteorology.  fODS_LBC isolates the effect of stratospheric ozone decreases on the
287　tropospheric ozone budget, but also shows that the effect of circulation changes has been significant.  The
288　behavior of the STE term in fODS_LBC shows that the faster Brewer-Dobson circulation and increased mass
289　flux to the troposphere are also important controls on the budget.  The two experiments also show that there is
290　enhanced NCP in HIST, and that this offsets a significant decrease in ozone transport via STE, and thus
291　moderates the effect of decreased stratospheric ozone on tropospheric ozone burden.
292
293
294

## Summary

296　Between 1979 and ~1994 there is an increase in NCP of tropospheric ozone in response to increases in
297　anthropogenic ozone precursors and an indirect decrease in transport to the troposphere which is the result of
298　stratospheric ozone depletion caused by halogenated ODS. These drivers are in opposition, similar in
299　magnitude, and are moderated by the change in chemical loss, resulting in a slight decrease in the tropospheric
300　ozone burden despite increases to ozone precursor emissions.  From 1994 to 2006, the tropospheric ozone
301　burden has been increasing, driven by decreases to NCP again being offset by changes to STE. These drivers of
302　tropospheric ozone, which are in opposition, turn out to be of similar magnitude, leading to a near-cancelling
303　behaviour in changes to the budget terms and so a smaller change in ozone than in the $P_{O3}$, $L_{O3}$ or STE terms
304　that control it.
305
306　Over the recent historical period, our study demonstrates that stratospheric ozone depletion has had a large
307　impact on tropospheric ozone.  Without the resulting decrease of STE, the large increase in NCP over the period
308　1979-1994 would have increased the tropospheric ozone burden.  After 1994, there is a levelling off in the
309　growth of emissions, and, coincidentally, a slight increase in STE, which together serve to increase the
310　tropospheric ozone burden.
311
312　Our study uses two complementary methods to diagnose the stratospheric input.  Our chemical budget
313　diagnostics allow us to identify a residual term, which we ascribe to STE.  Separately, we use dynamical
314　methods to determine the amount of stratospheric ozone transported to the troposphere.  We show that these two
315　methods agree to within 2%, lending confidence to our analysis of the impact of stratospheric transport on
316　tropospheric ozone.
317
318　Our results highlight the role of the stratosphere on tropospheric composition, and the utility of whole-
319　atmosphere chemistry schemes with interactive stratospheric chemistry.  Comparison with other UKCA models
320　in the CCMI project, highlights the critical role of tropospheric NMVOC chemistry in model skill.  Finally, our
321　results demonstrate the importance of STT on present (Neu et al., 2014) and future tropospheric ozone (Sekiya
322　& Sudo, 2014), particularly as stratospheric ozone recovers over this century.  This will be  particularly
323　important in regions affected by downward transport, e.g. NH midlatitudes in springtime (Lin et al., 2015).  The
324　complicating effects of circulation changes (see Polvani et al. (2018)  necessitate further study at the regional
325　scale using a dynamical model with interactive chemistry to fully understand the implications of stratospheric
326　ozone recovery on tropospheric composition, radiative forcing and air quality.
327

## Acknowledgements

# References

Abalos, M., Polvani, L., Calvo, N., Kinnison, D., Ploeger, F., Randel, W., & Solomon, S. (2019). New Insights on the Impact of Ozone-Depleting Substances on the Brewer-Dobson Circulation. *Journal of Geophysical Research: Atmospheres*, *124*(5), 2435–2451. https://doi.org/10.1029/2018JD029301

Archibald, Alexander T., O'Connor, F. M., Abraham, N. L., Archer-Nicholls, S., Chipperfield, M. P., Dalvi, M., et al. (2019). Description and evaluation of the UKCA stratosphere-troposphere chemistry scheme (StratTrop vn 1.0) implemented in UKESM1. *Geoscientific Model Development Discussions*, 1–82. https://doi.org/10.5194/gmd-2019-246

Butchart, N. (2014). The Brewer-Dobson circulation. *Reviews of Geophysics*, *52*(2), 157–184. https://doi.org/10.1002/2013RG000448

Dee, D. P., Uppala, S. M., Simmons, A. J., Berrisford, P., Poli, P., Kobayashi, S., et al. (2011). The ERA-Interim reanalysis: configuration and performance of the data assimilation system. *Quarterly Journal of the Royal Meteorological Society*, *137*(656), 553–597. https://doi.org/10.1002/qj.828

Dhomse, S. S., Kinnison, D., Chipperfield, M. P., Salawitch, R. J., Cionni, I., Hegglin, M. I., et al. (2018). Estimates of ozone return dates from Chemistry-Climate Model Initiative simulations. *Atmospheric Chemistry and Physics*, *18*(11), 8409–8438. https://doi.org/10.5194/acp-18-8409-2018

Eyring, V., Lamarque, J. ‐ F., Hess, P., Arfeuille, F., Bowman, K., Chipperfield, M. P., et al. (2013). Overview of IGAC/SPARC Chemistry ‐ Climate Model Initiative (CCMI) community simulations in support of upcoming ozone and climate assessments, SPARC Newsletter 40.

Gaudel, A., Cooper, O. R., Ancellet, G., Barret, B., Boynard, A., Burrows, J. P., et al. (2018). Tropospheric Ozone Assessment Report: Present-day distribution and trends of tropospheric ozone relevant to climate and global atmospheric chemistry model evaluation. *Elem Sci Anth*, *6*(1), 39. https://doi.org/10.1525/elementa.291

Granier, C., Bessagnet, B., Bond, T., D'Angiola, A., Denier van der Gon, H., Frost, G. J., et al. (2011). Evolution of anthropogenic and biomass burning emissions of air pollutants at global and regional scales during the 1980–2010 period. *Climatic Change*, *109*(1), 163. https://doi.org/10.1007/s10584-011-0154-1

Griffiths, P.; Keeble, J.; Shin, Y.; Abraham, L.; Archibald, A.; Pyle, J. (2020): WCRP CCMI-1: UM-UKCA output following the CCMI refC1SD experiment protocol. Centre for Environmental Data Analysis, 2020. https://catalogue.ceda.ac.uk/uuid/549bce914f66451d838bff5c0a557b37

Hewitt, H. T., Copsey, D., Culverwell, I. D., Harris, C. M., Hill, R. S. R., Keen, A. B., et al. (2011). Design and implementation of the infrastructure of HadGEM3: the next-generation Met Office climate modelling system. *Geoscientific Model Development*, *4*(2), 223–253. https://doi.org/10.5194/gmd-4-223-2011

Karset, I. H. H., Berntsen, T. K., Storelvmo, T., Alterskjær, K., Grini, A., Olivié, D., et al. (2018). Strong impacts on aerosol indirect effects from historical oxidant changes. *Atmospheric Chemistry and Physics*, *18*(10), 7669–7690. https://doi.org/10.5194/acp-18-7669-2018

Keeble, J., Braesicke, P., Abraham, N. L., Roscoe, H. K., & Pyle, J. A. (2014). The impact of polar stratospheric ozone loss on Southern Hemisphere stratospheric circulation and climate. *Atmospheric Chemistry and Physics*, *14*(24), 13705–13717. https://doi.org/10.5194/acp-14-13705-2014

378    Keeble, James, Brown, H., Abraham, N. L., Harris, N. R. P., & Pyle, J. A. (2018). On ozone trend detection: using
379        coupled chemistry–climate simulations to investigate early signs of total column ozone recovery.
380        *Atmospheric Chemistry and Physics*, *18*(10), 7625–7637. https://doi.org/10.5194/acp-18-7625-2018

381    Lin, M., Fiore, A. M., Horowitz, L. W., Langford, A. O., Oltmans, S. J., Tarasick, D., & Rieder, H. E. (2015).
382        Climate variability modulates western US ozone air quality in spring via deep stratospheric intrusions.
383        *Nature Communications*, *6*(1). https://doi.org/10.1038/ncomms8105

384    Maeder, J. A., Staehelin, J., Peter, T., Brunner, D., Rieder, H. E., and Stahel, W. A.: Evidence for the effectiveness
385        of the Montreal Protocol to protect the ozone layer, Atmos. Chem. Phys., 10, 12161– 12171,
386        https://doi.org/10.5194/acp-10-12161-2010, 2010.

387    Monks, P. S., Archibald, A. T., Colette, A., Cooper, O., Coyle, M., Derwent, R., et al. (2015). Tropospheric ozone
388        and its precursors from the urban to the global scale from air quality to short-lived climate forcer.
389        *Atmospheric Chemistry and Physics*, *15*(15), 8889–8973. https://doi.org/10.5194/acp-15-8889-2015

390    Morgenstern, O., Braesicke, P., O'Connor, F. M., Bushell, A. C., Johnson, C. E., Osprey, S. M., & Pyle, J. A.
391        (2009). Evaluation of the new UKCA climate-composition model – Part 1: The stratosphere.
392        *Geoscientific Model Development*, *2*(1), 43–57. https://doi.org/10.5194/gmd-2-43-2009

393    Morgenstern, Olaf, Hegglin, M. I., Rozanov, E., O&amp;apos;Connor, F. M., Abraham, N. L., Akiyoshi, H., et
394        al. (2017). Review of the global models used within phase 1 of the Chemistry–Climate Model Initiative
395        (CCMI). *Geoscientific Model Development*, *10*(2), 639–671. https://doi.org/10.5194/gmd-10-639-2017

396    Myhre, G., Shindell, D., Bréon, F.-M., Collins, W., Fuglestvedt, J., Huang, J., et al. (2013). Anthropogenic and
397        Natural Radiative Forcing. In T. F. Stocker, D. Qin, G.-K. Plattner, M. Tignor, S. K. Allen, J. Boschung,
398        et al. (Eds.), *Climate Change 2013: The Physical Science Basis. Contribution of Working Group I to the
399        Fifth Assessment Report of the Intergovernmental Panel on Climate Change* (pp. 659–740). Cambridge,
400        United Kingdom and New York, NY, USA: Cambridge University Press.
401        https://doi.org/10.1017/CBO9781107415324.018

402    Naik, V., Voulgarakis, A., Fiore, A. M., Horowitz, L. W., Lamarque, J.-F., Lin, M., et al. (2013). Preindustrial to
403        present-day changes in tropospheric hydroxyl radical and methane lifetime from the Atmospheric
404        Chemistry and Climate Model Intercomparison Project (ACCMIP). *Atmospheric Chemistry and Physics*,
405        *13*(10), 5277–5298. https://doi.org/10.5194/acp-13-5277-2013

406    Neu, J. L., Flury, T., Manney, G. L., Santee, M. L., Livesey, N. J., & Worden, J. (2014). Tropospheric ozone
407        variations governed by changes in stratospheric circulation. *Nature Geoscience*, *7*(5), 340–344.
408        https://doi.org/10.1038/ngeo2138

409    O'Connor, F. M., Johnson, C. E., Morgenstern, O., Abraham, N. L., Braesicke, P., Dalvi, M., et al. (2014).
410        Evaluation of the new UKCA climate-composition model – Part 2: The Troposphere. *Geoscientific
411        Model Development*, *7*(1), 41–91. https://doi.org/10.5194/gmd-7-41-2014

412    Polvani, L. M., Abalos, M., Garcia, R., Kinnison, D., & Randel, W. J. (2018). Significant Weakening of Brewer-
413        Dobson Circulation Trends Over the 21st Century as a Consequence of the Montreal Protocol.
414        *Geophysical Research Letters*, *45*(1), 401–409. https://doi.org/10.1002/2017GL075345

415    Prather, M. J. (2009). Tropospheric O3 from photolysis of O2. *Geophysical Research Letters*, *36*(3).
416        https://doi.org/10.1029/2008GL036851

417 Rayner, N. A., Parker, D. E., Horton, E. B., Folland, C. K., Alexander, L. V., Rowell, D. P., et al. (2003). Global
418         analyses of sea surface temperature, sea ice, and night marine air temperature since the late nineteenth
419         century. *Journal of Geophysical Research: Atmospheres*, *108*(D14).
420         https://doi.org/10.1029/2002JD002670

421 Revell, L. E., Stenke, A., Tummon, F., Feinberg, A., Rozanov, E., Peter, T., et al. (2018). Tropospheric ozone in
422         CCMI models and Gaussian process emulation to understand biases in the SOCOLv3 chemistry–climate
423         model. *Atmospheric Chemistry and Physics*, *18*(21), 16155–16172. https://doi.org/10.5194/acp-18-
424         16155-2018

425 Sekiya, T., & Sudo, K. (2014). Roles of transport and chemistry processes in global ozone change on interannual
426         and multidecadal time scales. *Journal of Geophysical Research: Atmospheres*, *119*(8), 4903–4921.
427         https://doi.org/10.1002/2013JD020838

428 Stevenson, D. S., Dentener, F. J., Schultz, M. G., Ellingsen, K., Noije, T. P. C. van, Wild, O., et al. (2006).
429         Multimodel ensemble simulations of present-day and near-future tropospheric ozone. *Journal of
430         Geophysical Research: Atmospheres*, *111*(D8). https://doi.org/10.1029/2005JD006338

431 Telford, P. J., Braesicke, P., Morgenstern, O., & Pyle, J. A. (2008). Technical Note: Description and assessment
432         of a nudged version of the new dynamics Unified Model. *Atmospheric Chemistry and Physics*, *8*(6),
433         1701–1712. https://doi.org/10.5194/acp-8-1701-2008

434 Tilmes, S., Lamarque, J.-F., Emmons, L. K., Kinnison, D. E., Marsh, D., Garcia, R. R., et al. (2016).
435         Representation of the Community Earth System Model (CESM1) CAM4-chem within the Chemistry-
436         Climate Model Initiative (CCMI). *Geoscientific Model Development*, *9*(5), 1853–1890.
437         https://doi.org/10.5194/gmd-9-1853-2016

438 Voulgarakis, A., Hadjinicolaou, P., & Pyle, J. A. (2011). Increases in global tropospheric ozone following an El
439         Niño event: examining stratospheric ozone variability as a potential driver. *Atmospheric Science Letters*,
440         *12*(2), 228–232. https://doi.org/10.1002/asl.318

441 Voulgarakis, A., Naik, V., Lamarque, J.-F., Shindell, D. T., Young, P. J., Prather, M. J., et al. (2013). Analysis of
442         present day and future OH and methane lifetime in the ACCMIP simulations. *Atmospheric Chemistry
443         and Physics*, *13*(5), 2563–2587. https://doi.org/10.5194/acp-13-2563-2013

444 Voulgorakis, A., Shindell, D.T., and Faluvegi, G. Linkages between ozone-depleting substances, tropospheric
445         oxidation and aerosols, Atmos. Chem. Phys., 13, 4907–4916, 2013

446 Wesely, M. L. (1989). Parameterization of surface resistances to gaseous dry deposition in regional-scale
447         numerical models. *Atmospheric Environment (1967)*, *23*(6), 1293–1304. https://doi.org/10.1016/0004-
448         6981(89)90153-4

449 Young, P. J., Archibald, A. T., Bowman, K. W., Lamarque, J.-F., Naik, V., Stevenson, D. S., et al. (2013). Pre-
450         industrial to end 21st century projections of tropospheric ozone from the Atmospheric Chemistry and
451         Climate Model Intercomparison Project (ACCMIP). *Atmospheric Chemistry and Physics*, *13*(4), 2063–
452         2090. https://doi.org/10.5194/acp-13-2063-2013

453 Young, P. J., Naik, V., Fiore, A. M., Gaudel, A., Guo, J., Lin, M. Y., et al. (2018). Tropospheric Ozone Assessment
454         Report: Assessment of global-scale model performance for global and regional ozone distributions,
455         variability, and trends. *Elem Sci Anth*, *6*(1), 10. https://doi.org/10.1525/elementa.265

456
457